行政院國家科學委員會補助專題研究計畫成果報告

混成式可調曲率環場視聽系統(3/3)－子計劃二：銀幕用矩陣式平面喇叭之研發

計畫主持人：白明憲　教授

中 華 民 國九十二年九月

行政院國家科學委員會補助專題研究計畫成果報告

※※※※※※※※※※※※※※※※※※※※※※※※※※※※※※

※ ※

※ 混成式可調曲率環場視聽系統(3/3)－子計劃二：銀幕用 ※

※ 矩陣式平面喇叭之研發 ※

※ ※

※※※※※※※※※※※※※※※※※※※※※※※※※※※※※※

計畫類別：□個別型計畫 ☑ 整合型計畫

計畫編號：NSC91－2212－E－009－032 91PFA0600071

執行期間： 91 年 8 月 1 日至 92 年 7 月 31 日

計畫主持人：白明憲 教授

計畫參與人員： 郭志挺、白淦元

本成果報告包括以下應繳交之附件：

□赴國外出差或研習心得報告一份

□赴大陸地區出差或研習心得報告一份

□出席國際學術會議心得報告及發表之論文各一份

□國際合作研究計畫國外研究報告書一份

執行單位：交通大學機械工程學系

中 華 民 國 92 年 9 月 15 日

Optimal Design and Implementation of an Omni-directional Panel Speaker Array Using the Genetic Algorithm

Mingsian R. Bai and Jihting Kuo

Department of Mechanical Engineering, National Chiao-Tung University, 1001 Ta-Hsueh Road, Hsin-Chu 300, Taiwan, ROC, Email: msbai@cc.nctu.edu.tw

Abstract

A panel speaker array with omni-directional radiation pattern is presented in this paper. Array signal processing techniques are utilized to manipulate the sound beam electronically such that wide angle radiation can be maintained over a large frequency range. In order to achieve this purpose without sacrificing the array efficiency, the genetic algorithm (GA) is employed in the design stage to calculate the optimal array coefficients. The GA proved to be an effective technique in searching for the array coefficients that maximize the efficiency with desired flatness of radiation pattern. In addition, a modified design is also proposed to further enhance the efficiency in the low frequency range. The resulting designs are implemented on a digital signal processor (DSP) platform and experimentally verified by using a small 5×1 panel speaker array and a large 3×3 panel speaker array.

Keywords: omni-directional radiation、genetic algorithm、array efficiency、flatness.

摘要：

本計劃欲設計一具有全向性聲壓輻射波束的矩陣式平面喇叭，我們利用陣列訊號處理的技術來對聲壓波束做全頻域全向性的處理，為了要達到此一目的且在不犧牲矩陣效能的前提下，使用基因演算法能夠有效地找尋到使系統達到最佳輻射波束平坦度的矩陣參數。除此之外，使用經過改良設計的矩陣參數可以有效地增加輻射波束在低頻範圍的效果。整個系統的實現是藉由一個小的 5×1 的矩陣式平面喇叭，和一個大的 3×1 的矩陣式平面喇叭，經由數位信號處理器（DSP）的運算所達到。

關鍵字：全向性輻射、基因演算法、陣列效能、平坦度。

TABLE OF CONTENTS

1 Introduction

This paper focused on the development of a panel speaker array with omni-directional radiation pattern. This array serves as a projection screen of an audio and video system that integrates the technologies of panel speakers, video projection, and array signal processing. This system is intended for the applications such as oral presentation, home theater, conferencing, public addressing, and so forth.

The main reason of using panel speakers lies in its flatness and compactness, which makes them well suited for the application such as the projection screen in our case. However, the randomly distributed flexural modes of a large panel create efficiency problem in low frequency and peculiar directivity in high frequency [1]. A possible solution to these problems associated with panel speakers is to break a large panel into smaller pieces and excite each element independently, using array signal processing techniques. This approach enables us to "control" the beam pattern of the generated sound field with more flexibility over the conventional single panel configuration. In particular, we seek in this work to generate an omni-directional response over a wide frequency range, using panel speaker arrays.

Figure 1 shows a linear speaker array and its signal processing unit. For a uniform linear array, it is well known that the directional response is the spatial Fourier transform of the array coefficients [2]. It is then straightforward to obtain a frequency-invariant, omni-directional array by using inverse Fourier transform. However, the omni-directionality is generally achieved at the expense of array efficiency. The array coefficients resulting from inverting perfect spectral flatness tend to be an impulse function in the spatial domain, which implies only one element in the array is active and the remaining elements are at rest. Instead of the above naïve approach, a method of optimization was employed in this paper to calculate the

array coefficients that attain optimal efficiency with a desired directional response, or spectral flatness in the transformed domain. Due to the highly nonlinear nature of the array optimization problem, this study employs an optimization technique, the genetic algorithm (GA), to effectively search the global optimum in a nonlinear space with a large number of parameters. Typically, there are $2(2N+1)$ parameters, including the magnitudes and phases, to determine for an array with $2N+1$ elements. Thus, the search space can be very large for a moderate number of array elements. The GA is well suited to dealing with such optimization problem. Reference [3] optimized a linear array and a planar array using GA to produce beam patterns with the lowest side lobe level. A GA-based technique is proposed in this paper for finding array coefficients to maximize two cost functions: spectral flatness and array efficiency. In addition to the basic version, a modified design is also proposed to further enhance the efficiency in the low frequency range. These two optimal designs are referred in this paper as the omni-directional array and the modified omni-directional array.

In order to verify the proposed optimal array designs, experiments were carried out in this research. A small 5×1 panel speaker array and a large 3×3 panel speaker array were constructed for experimental verification. Signal processing and electronic compensation are carried out by using a multi-channel digital signal processor (DSP). Results obtained using the optimal designs will be discussed with reference to an uncompensated array.

2 Fundamentals of Uniformly Linear Arrays

The array configuration employed in this work is the uniformly linear array (ULA) in which array elements are equally spaced in a straight line. Some fundamentals of ULA relevant to the ensuing discussion are given in this section.

2.1 The Far-field Model of a ULA

Consider the ULA with $2N+1$ elements, as shown in Fig. 1(a). The observation point is assumed in the far-field such that $r >> 2Nd$, where d is the spacing between two adjacent elements, r is the distance between the observation point and the array center. As a rule of thumb, the far field begins at the distance three times the characteristic dimension of the source [4] or, in our case, $2Nd$. The sound pressure of this array is given by [5]

$$P(f,\theta,r) = A(f,\theta)R(f,r)B(f,\theta), \tag{1}$$

where f is the frequency of the source, θ is the angle measured from the normal of the array, $A(f,\theta)$ is the directional response of a single array element, and $R(f,r) = r^{-1}\exp(j2\pi fr/c)$ represents the spherical spreading. The beam pattern $B(f,\theta)$ is expressed as

$$B(f,\theta) = \sum_{n=-N}^{N} g_n(f) e^{jn\frac{2\pi fd\sin\theta}{c}}, \tag{2}$$

where $g_n(f)$ is the array coefficient of the nth element and c is the speed of sound.

We further restrict the array coefficients $g_n(f)$ to be frequency-independent complex constants, g_n. Then the beam pattern can be written as

$$B(u) = \sum_{n=-N}^{N} g_n e^{jnu}, \tag{3}$$

where $u = 2\pi fd\sin\theta/c$ is a non-dimension angle. Inspection of Eq. (3) reveals that the beam pattern is essentially the frequency response of a FIR filter with coefficients g_n. Thus, the design problem of an omni-directional array can be regarded as the design of an all-pass FIR filter.

2.2 Characteristics of a ULA

Analogous to time-domain filters, a ULA is a filter in the spatial domain, where

the wave number k is the spatial frequency, the spacing d is the spatial sampling period, and the non-dimensional angle u is the digital spatial frequency. Increase of the array aperture will result in the decrease of the beam width and thus improved resolution.

The beam pattern of a typical ULA is shown in Fig. 2. The non-dimensional angle, $u = 2\pi f d \sin\theta / c$, is a nonlinear function of the look angle θ. The *beam-broadening effect* arises as θ varies from 0° to ±90°. When the main beam of an array is steered to θ_0, its beam width can be approximated as [2]

$$2\Delta\theta \approx 2\frac{\lambda_c}{(2N+1)d\cos\theta_0}, \tag{4}$$

where $\Delta\theta$ is the angle difference between the look angle θ_0 and the adjacent null point and λ_c is the source wave length.

The physical limits of the look angle $\theta = \pm 90°$ correspond to the non-dimensional angle $u_0 = \pm kd$, which in turn increases with increasing frequency f. Note that the parameter u_0 is then likely to be greater than π above certain frequency. In this case, grating lobes will appear within the observation range. To avoid the grating lobes, the spacing d is generally chosen according to

$$d \le \frac{\lambda}{2}, \tag{5}$$

where $\lambda = c/f$ is the wave length and c is the sound speed.

2.3 Omni-directional Response

As mentioned previously, the goal of this work is to design speaker arrays with omni-directional characteristics. Some considerations with regard to this aspect are addressed as follows. The dash line in Fig. 3 shows a typical omni-directional beam pattern plotted in the u-domain. The smaller are the ripples, the closer is the array to the ideally omni-directional response. Since the parameter u is non-dimensional, the

omni-directional response applies to all frequencies.

The array efficiency can be further enhanced by taking advantage of a subtle point in the omni-directional response. With reference to Fig. 3, it can happen that in low frequency the effective range of the look angle gives a range of the non-dimensional angle less than $\pm\pi$, i.e., $u_0=kd<\pi$. The regions [π, $-kd$) and (kd, π] are virtually "invisible." It would be waste to provide energy in invisible regions (shadow areas) because in those regions no sound radiation will physically exist. Alternatively, it is more desirable to design a band-pass array pattern (solid line in Fig. 3), concentrating within the "visible" region, $[-\pi, \pi]$, such that the overall efficiency can be improved. In next section, a phase compensation scheme will be presented to produce omni-directional pattern, while at the same time prevent the design effort being wasted in the invisible region.

3 Optimization Schemes for Omni-directional Arrays

In this section, optimization schemes is presented to achieve a better compromise between array efficiency and the omni-directional response for the panel speaker array.

3.1 The preliminary Scheme

Let the autocorrelation function be

$$R(k)=\sum_{n=-\infty}^{\infty} g_n g_{k-n}^{*}, \tag{6}$$

where g_n if the array gain for the nth element and "*" denotes complex conjugate [6]. The power spectrum is given by

$$S(u)=\|B(u)\|_2^2, \tag{7}$$

where $\|\ \|_2$ denotes the 2-norm. It is well known that the power spectrum is the

Fourier transform of the autocorrelation function

$$S(u) = \sum_{k=-\infty}^{\infty} R(k) e^{-jku} . \tag{8}$$

Assume the array is of $2N+1$ elements. The first performance index employed in the optimization procedure is the "array efficiency"

$$\eta = \frac{R(0)}{(2N+1)|\mathbf{g}|_{\infty}}, \tag{9}$$

where $\mathbf{g} = \{g_n \mid -N \le n \le N, n \in N\}$, $|\mathbf{g}|_{\infty} = \max\{g_n \mid -N \le n \le N\}$ is the infinity norm of **g**, and

$$R(0) = \sum_{n=-N}^{N} |g_n|^2 = \frac{1}{2\pi} \int_{-\pi}^{\pi} S(u) du , \tag{10}$$

where the Parseval theorem has been invoked. Thus, the array efficiency can be interpreted as the mean-square spectrum normalized by $|\mathbf{g}|_{\infty}$. The array efficiency will be close to unity if all array elements are active.

Using Eq. (8), we have

$$\frac{1}{2\pi} \int_{-\pi}^{\pi} S(u) du = \int_{-\pi}^{\pi} \sum_{k=-2N}^{2N} R(k) e^{jku} du = R(0) . \tag{11}$$

By the Parseval's relation,

$$\sum_{k=-2N}^{2N} |R(k)|^2 = \frac{1}{2\pi} \int_{\pi}^{\pi} S^2(u) du . \tag{12}$$

Define the "merit factor" as [7]

$$F_a = \frac{R^2(0)}{\sum_{k \neq 0} |R(k)|^2} . \tag{13}$$

Substituting Eqs. (11) and (12) into Eq. (13) yields

$$F_a = \frac{\left(\int_{-\pi}^{\pi} S(u) du \right)^2}{2\pi \int_{-\pi}^{\pi} [S^2(u) - R^2(0)] du} , \tag{14}$$

The denominator of F_a can also be written as

$$\int_{-\pi}^{\pi}[S^2(u)-R^2(0)]du=\int_{-\pi}^{\pi}[S(u)-R(0)]^2du \tag{15}$$

Thus, the merit factor F_a can be interpreted as the ratio of the mean-square spectrum over the spectral variance. The mean-square spectrum can be related to the efficiency of the array, whereas the spectral variance can be related to the spectral flatness. It is then most desirable to have an array with a large merit factor, i.e., high efficiency and small variance. However, there is generally a tradeoff between these two indices, which entails for the need of an optimization procedure to best accomplish this tradeoff.

3.2 The Modified Scheme

It is mentioned previously that, in low frequency $u_0=2\pi f_0 d/c < \pi$, energy can be wasted in the invisible region. To avoid this pitfall, we thus modify Eq. (14) to concentrate the design effort on only the visible region $[-u_0, u_0]$. The modified merit factor F_b is written as

$$F_b=\frac{\left(\int_{-u_0}^{u_0}S(u,f_0)du\right)^2}{2u_0\int_{-u_0}^{u_0}[S(u,f_0)-\mu_s]^2du}, \tag{16}$$

where

$$\mu_s=\frac{1}{2u_0}\int_{-u_0}^{u_0}S(u,f_0)du \tag{17}$$

Equation (17) can be expressed as

$$\mu_s=\frac{1}{2u_0}\int_{-u_0}^{u_0}\sum_{k=-\infty}^{\infty}[R(k)e^{jku}]du$$

With some manipulations, above equation can be rewritten as

$$\mu_s=\frac{1}{2u_0}\sum_{k=-\infty}^{\infty}[R(k)\frac{2\sin(ku_0)}{k}] \tag{18}$$

It can be shown the following relations are valid

$$g_n \xleftrightarrow{FT} B(u),$$

$$R(k) \xleftrightarrow{FT} S(u), \quad S(u) = B(u)B^*(u),$$

$$C(k) \xleftrightarrow{FT} S^2(u), \quad S^2(u) = S(u)S^*(u),$$

where

$$C(k) = \sum_{n=-\infty}^{\infty} R(n)R^*(k-n)$$

and FT denotes the Fourier transform. Thus, by the above Fourier relations

$$S^2(u) = \sum_{k=-\infty}^{\infty} C(k)e^{iku}. \tag{19}$$

Define

$$G_s = \frac{1}{2u_0}\int_{-u_0}^{u_0} S^2(u, f_0)du \tag{20}$$

From Eqs. (17)-(19), Eq. (20) can be expressed as

$$G_s = \frac{1}{2u_0}\sum_{k=-\infty}^{\infty}[C(k)\frac{2\sin(ku_0)}{k}], \tag{21}$$

With some manipulations, the denominator of F_b in Eq. (16) can be written as

$$2u_0\int_{-u_0}^{u_0}[S(u, f_0) - \mu_s]^2 du = 4u_0^2 G_s - 4u_0^2\mu_s^2.$$

Equation (16) is now summarized as

$$F_b = \frac{\left(\int_{-u_0}^{u_0} S(u, f_0)du\right)^2}{2u_0\int_{-u_0}^{u_0}[S(u, f_0) - \mu_s]^2 du} = \frac{\mu_s^2}{G_s - \mu_s^2}. \tag{22}$$

4 Genetic Algorithm

The genetic algorithm (GA) is an optimization algorithm based on the theory of biological evolution [8]. The GA is particularly useful for solving complex and non-convex problem in discrete space with a large number of parameters. The main difference between the GA and the other search algorithms is that the GA operates on

a "population" of strings (chromosomes) instead of a single starting point. Each chromosome is associated with a "fitness" value as the performance measure. The GA forms "generations" of solution candidates and attempts to maximize the total fitness of each generation. Owing to the multiple starting point nature of the algorithm, the GA is less unlikely to be trapped in a local optimum than many other optimization methods.

4.1 Design Procedure of the GA

The first step of the GA is to encode the input parameters for the fitness function into binary numbers. As shown in Fig. 4, the array coefficients $g_n = a_n e^{j\phi_n}$, n=-N,-N+1, ..., N-1, N, are encoded in a r-bit discrete space. Then all coefficients are concatenated to form a binary string called a chromosome. The corresponding fitness value is computed.

The flowchart of the array design using GA is shown in Fig. 5. To initialize the GA procedure, M individuals are randomly generated to form the first generation. In a GA cycle, three types of operators are invoked.

Reproduction: Each individual in the current population has a possibility of being selected to form the next generation according to the fitness. The probability to be selected for the kth chromosome is

$$p_k = \frac{f_k - f_{\min}}{\sum_{i=1}^{M} (f_i - f_{\min})}, \tag{23}$$

where f_i indicates the fitness function of the ith chromosome, and f_{min} indicates the minimum fitness value in the M chromosomes.

Crossover: With the crossover probability p_c, this step copies data from two parent individuals generated in the previous step to form new child solutions. The method

used in this paper is the *double point* crossover, where the two points are randomly chosen, as shown in Fig. 6(a). This splits each parent into three segments. The first child solution is formed by randomly copying each segment from either of the parents. The second child solution is formed from the segments not used by the first child. The parents are then replaced by their offsprings.

Mutation: This step is performed on each the chromosome according to the mutation probability p_m by randomly altering chromosomes, as shown in Fig. 6(b). The mutation probability p_m must be chosen appropriately. If p_m is too large, the GA will diverge. Conversely, if p_m is too small, the GA will terminate prematurely.

4.2 Application of the GA to the Array Design Problem

The parameters for the GA in our array design problem are

$$g_n = a_n e^{j\phi_n}, \quad n = -N, \cdots, N \tag{24}$$

where g_n is a complex constant, and a_n, ϕ_n are the magnitude and phase.

First, M sets of array coefficients a_n, ϕ_n are randomly generated. The ranges of the magnitude a_n and the phase ϕ_n are

$0 \le a_n \le 1$ and $0 \le \phi_n \le 2\pi$

Then, divide the full range into 2^r levels according to the desired resolutions and round the coefficients into the nearest integer. Encode the coefficients a_n and ϕ_n into r-bit binary representations. Then the binary codes of all $2(2N+1)$ coefficients are concatenated to form a chromosome. The objective of the GA is to optimize the array efficiency under the constraint of a desired spectral flatness.

4.3 Constraints

In order to ensure uniqueness of solutions, two fundamental constraints must be

incorporated into the optimization procedure. The first constraint pertains to the scaling of the array pattern. In order to simplify the formulation, we assume that the gain of the center element is unity.

$$g_0 = 1, \text{ and } |g_k| \le 1, \text{ where } -N \le k \le N, \ k \in N. \tag{25}$$

The second constraint pertains to the rotation of the array pattern. To avoid non-unique solutions due to rotation, the following constraint applies

$$\angle g_0 = \angle g_1 = 0 \tag{26}$$

To further simplify the formulation, the magnitudes of the array coefficients are assumed to be symmetric about the center element.

$$|g_{-N}| = |g_N|, \ |g_{-N+1}| = |g_{N-1}|, \ \ldots\ldots, \ |g_{-1}| = |g_1|. \tag{27}$$

5 Verification of the GA-based Array Design

5.1 Numerical Simulation

A simulation was carried out for the omni-directional array, using the preliminary scheme. With reference to the fitness function in Eq. (13), we choose M = 200, r = 16, and N = 6 in the simulation. Hence, 6 magnitude parameters and 11 phase parameters of array elements are arranged into one chromosome. The probabilities of crossover and mutation are set to be 0.85 and 0.01, separately. After approximately 300 iterations (20 minutes), the GA reached a maximum. The learning curve is shown in Fig. 7 and the results found by GA are summarized in Table 1. We compare the GA solution with the quadratic phase array (QPA) [4] in Fig 8. The GA design produced flatter array pattern than the QPA design with identical array efficiency.

Next, the modified scheme is investigated. The fitness function in Eq. (22) is used in the GA procedure. Choose $u_0 = 1.5$ and $N = 2$ in the optimization program. Simulated beam pattern using optimal array coefficients is shown in Fig. 9. Using the modified scheme, we are able to concentrate the beam pattern in the visible region, $u = -1.5 \sim 1.5$. This enhancement of efficiency is obtained for the frequency

$$f < \frac{u_0 c}{2\pi d} \tag{28}$$

For a frequency 1123 Hz satisfying the above relation, we compare the beam patterns between the two designs using the preliminary scheme and the modified scheme, respectively. The spacing $d = 6.7$ cm. The results in Fig. 10 show that the array using modified scheme gives larger output than the array using the preliminary scheme.

The array coefficients $g_{n,1}, g_{n,2}, \ldots, g_{n,m}$ of the nth element that is applicable to broadband signals can be obtained by repeating the GA procedures for each frequency, $f_1, f_2, \ldots, f_m$. For $f < c/2d$, both schemes can be used, whereas for $f > c/2d$ only the preliminary scheme is needed. The complex coefficients $g_{n,1}, g_{n,2}, \ldots, g_{n,m}$ amount to the frequency response function, based on which digital filters can be designed for each array element.

5.2 Experimental Investigation

A small 5×1 linear panel speaker array and a large 3x3 panel speaker matrix are constructed for experimental verification. The dimensions of the small panels are 7cm×6.7cm and the dimensions of the large panels are 30cm×30cm. The spacing d is 6.7cm in the 5×1 array and 30cm in the 3×3 matrix. The resulting designs are implemented on a digital signal processor (DSP) platform. All measurements were conducted inside a 3mx3mx4m anechoic chamber.

The first experiment pertains to the verification of the array design using the preliminary scheme of the GA procedure. Figure 11 shows the measured beam pattern of the 5×1 panel speaker array at the frequency 3 kHz. Figure 12 shows the measured beam pattern of the 3×3 panel speaker matrix at the frequency 1514 Hz. the results of these two figures illustrated omni-directional characteristics approximately from -60° to 60°.

The second experiment pertains to the verification of the array design using the modified scheme of the GA procedure. Figure 13 shows the measured beam pattern of the 5×1 panel speaker array at the frequency 1134 Hz. Figure 14 shows the measured beam pattern of the 3×3 panel speaker matrix at the frequency 879 Hz. From the experimental results, it is observed that the modified scheme of GA procedure indeed produced a design with higher level of output than the preliminary scheme.

6 Conclusions

It has been illustrated in this work that an omni-directional radiation pattern of panel speaker array can be achieved by using the GA-based optimization method. Both numerical and experimental investigations are carried out to justify the proposed techniques. A preliminary scheme and a modified scheme were developed to maximize the array efficiency under desired spectral flatness requirement. The GA proved to be an effective search technique for the current array design problem. In particular, the modified scheme is able to enhance the efficiency in frequency $f < \frac{c}{2d}$. The proposed GA procedure generally yields a satisfactory design within a short computational time. For the broadband case, both schemes can be combined to deal with different frequency ranges.

The resulting optimal designs are implemented on a DSP platform and are experimentally verified by using a small 5×1 panel speaker array and a large 3×3 panel speaker array. The experimental results indicate that the proposed GA techniques are able to produce an array design with omni-directional beam pattern. Between the two designs, the modified scheme yields more output by shifting the effort from the invisible region to the visible.

Although the ultimate goal of this work was to develop the large array, we were unable to verify its far-field behavior due to the limitation of current measuring environment. Much work is continuing in improving the implementation as well as measurement of the large array for future research.

Acknowledgments

Special thanks are due to the illuminating discussions with *NXT, New Transducers Limited*, UK. The work was supported by the *National Science Council* in Taiwan, under the project number NSC 89AFA06000714.

References

[1] M. R. Bai and T. Huang, "Development of Panel Loudspeaker System: Design, Evaluation and Enhancement," *J. Acoust. Soc. Am.* **109**, 2751-2761 (2001)

[2] D. F. Johnson and D. F. Dudgeon, *Array Signal Processing Concepts and Techniques* (Prentice Hall, Englewood Cliffs, NJ, 1993)

[3] R. L. Haupt, "Thinned Arrays Using Genetic Algorithms," *IEEE Trans. Antennas Propagation*, **42**, 993–999 (1994)

[4] D. L. Smith, "Discrete-Element Line Arrays — Their Modeling and Optimization," *J. Audio Eng. Soc.*, **45**, 949-964 (1997)

[5] R. M. Aarts and A. J. E. M. Janssen, "On Analytic Design of Loudspeaker Arrays

with Uniform Radiation Characteristics," *J. Acoust. Soc. Am.*, **107**, 287-292 (2000)

[6] G. F. M. Beenker, T. A. C. M. Claasen and P. W. C. Hermens, "Binary Sequences with a Maximally Flat Amplitude Spectrum," *Philips J. Res.*, **40**, 289-304 (1985)

[7] M. J. E. Golay, "The Merit Factor of Long, Low Autocorrelation Binary Sequences," *IEEE Trans. Inform. Theory*, **28**, 543 (1982)

[8] R. K. Belew and M. D. Vose, *Foundations of Genetic Algorithms* (Morgan Kaufmann Publishers, New York, 1997)

[9] G. L. Augspurger, "Near-Field and Far-Field Performance of Large Woofer Arrays," *J. Audio Eng. Soc.*, **38**, 231-236 (1990)

[10] D. G. Meyer, "Digital Control of Loudspeaker Array Directivity," *J. Audio Eng. Soc.*, **32**, 747-754 (1984)

[11] A. V. Oppenheim and R. W. Schafer, *Discrete-Time Signal Processing*, (Prentice Hall, Englewood Cliffs, NJ, 1989)

Table I. The array coefficients for the 13×1 optimal array (preliminary scheme) and the QPA array

Element index	Optimal array	QPA (z =18)
-6	0.13exp(j0.72)	0.74
-5	0.52exp(-j2.64)	-0.78
-4	0.64exp(-j0.29)	0.96
-3	0.53exp(j1.80)	-1.00
-2	1.00exp(-j1.81)	0.45
-1	0.87exp(j0.78)	0.67
0	1	-0.86
1	0.87	-0.67
2	1.00exp(j1.81)	0.45
3	0.53exp(j1.34)	1.00
4	0.64exp(j0.29)	0.96
5	0.52exp(-j0.50)	0.78
6	0.13exp(-j0.72)	0.74
Efficiency	0.63	0.63
Flatness	0.12	5.95

FIGURE LIST

FIG. 13 The measured beam patterns of the 5×1 panel speaker array in the frequency 1123 Hz. (dash line: preliminary scheme; solid line: modified scheme)

FIG. 14 The measured beam patterns of the 3×3 panel speaker matrix in the frequency 879 Hz. (dash line: preliminary scheme; solid line: modified scheme)

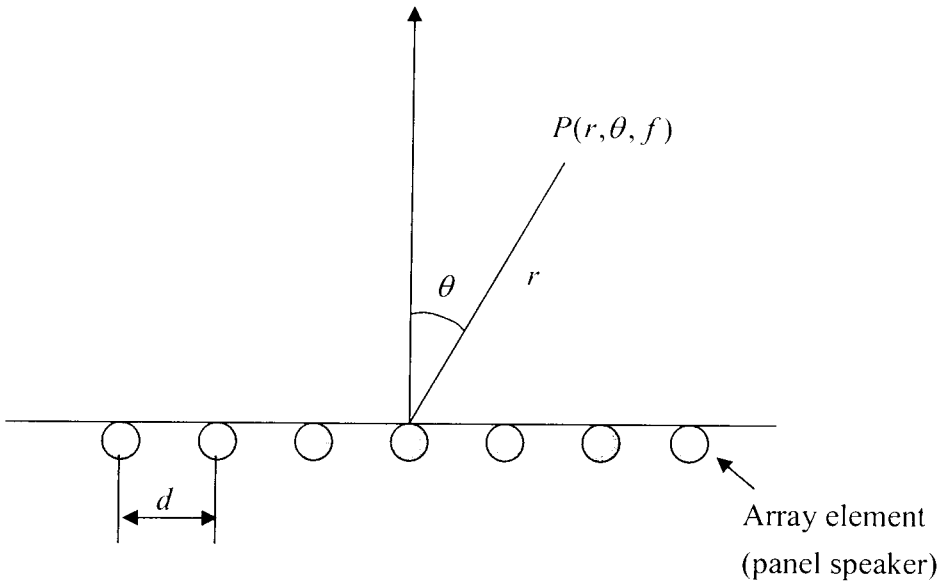

(a)

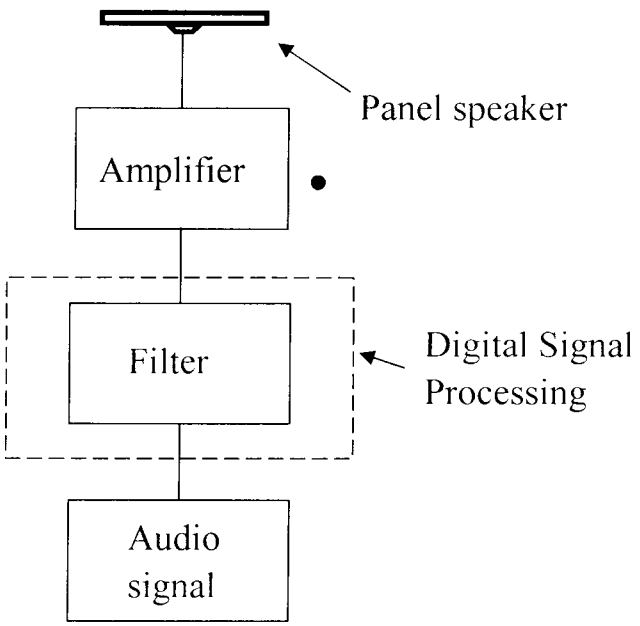

(b)

Fig. 1(a) and (b)
Bai and Kuo

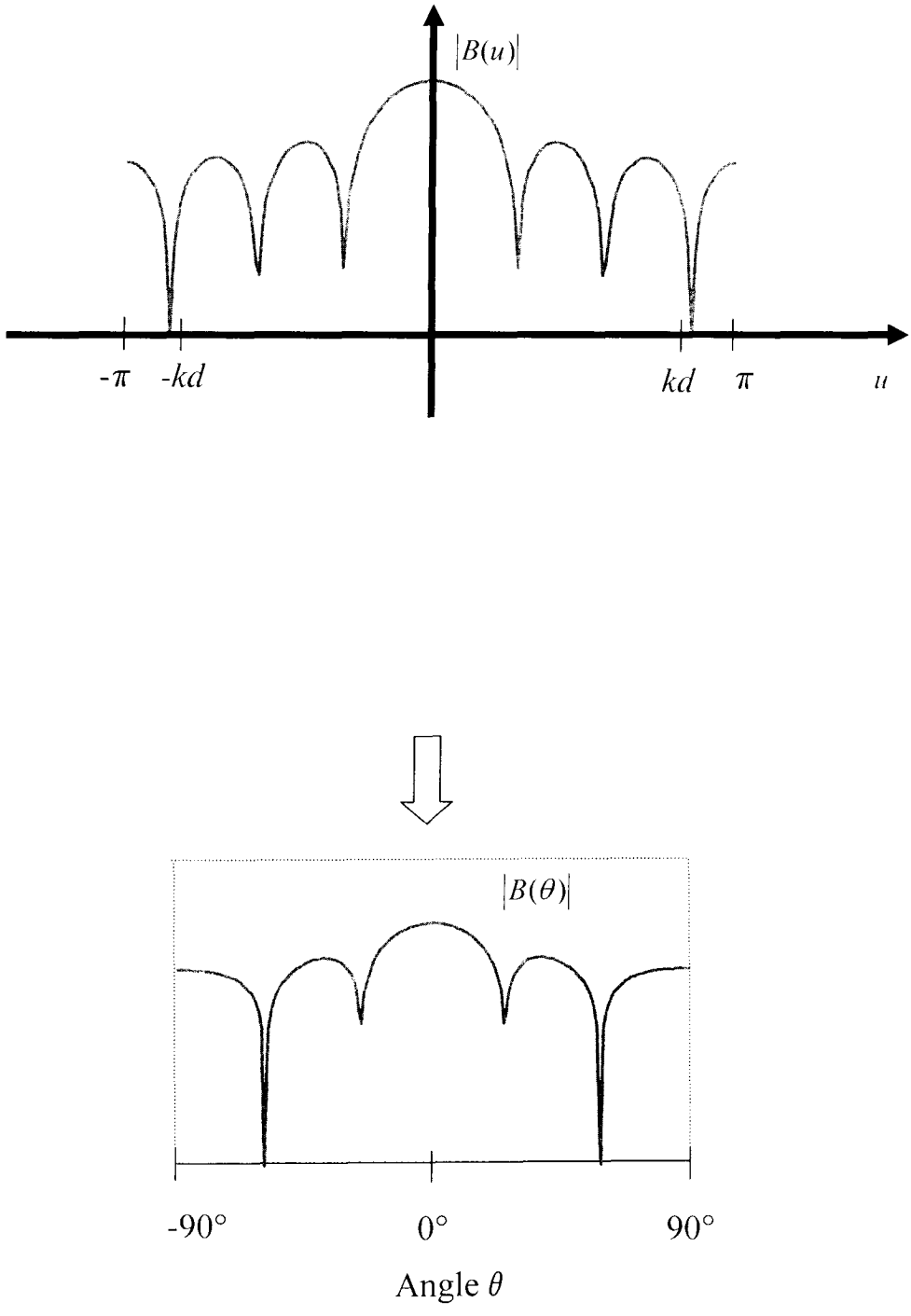

Fig. 2
Bai and Kuo

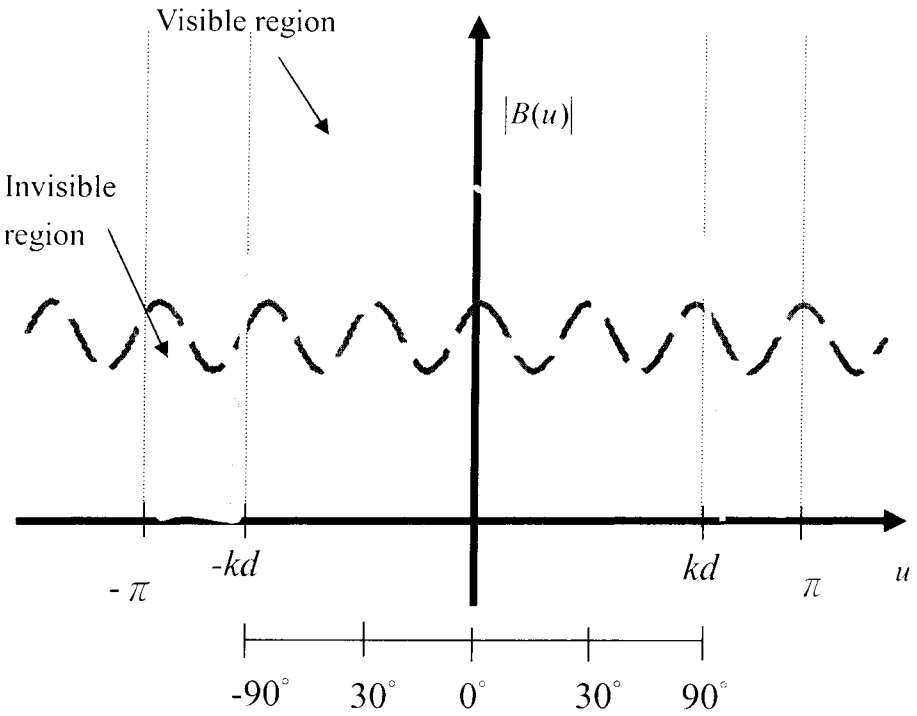

Fig. 3
Bai and Kuo

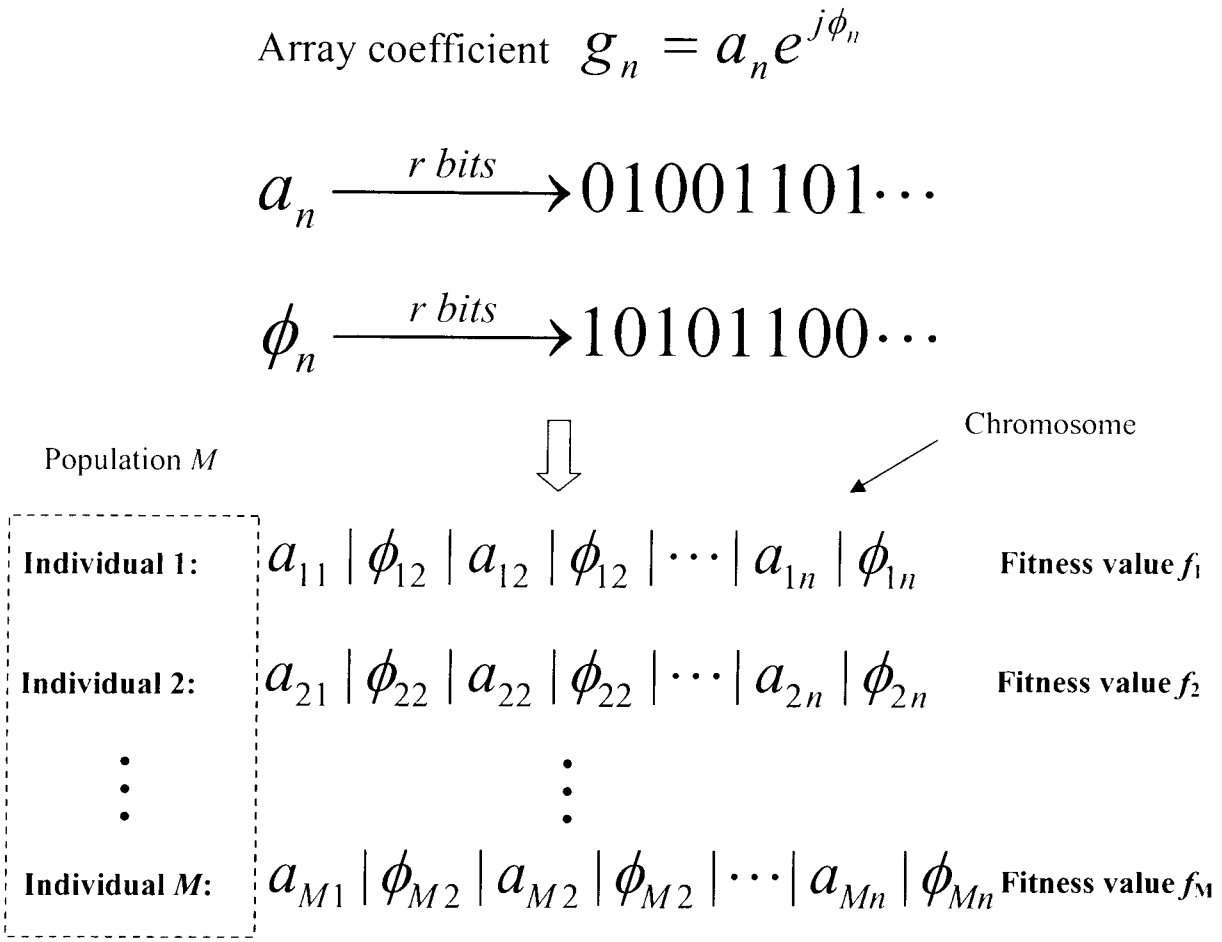

Fig. 4
Bai and Kuo

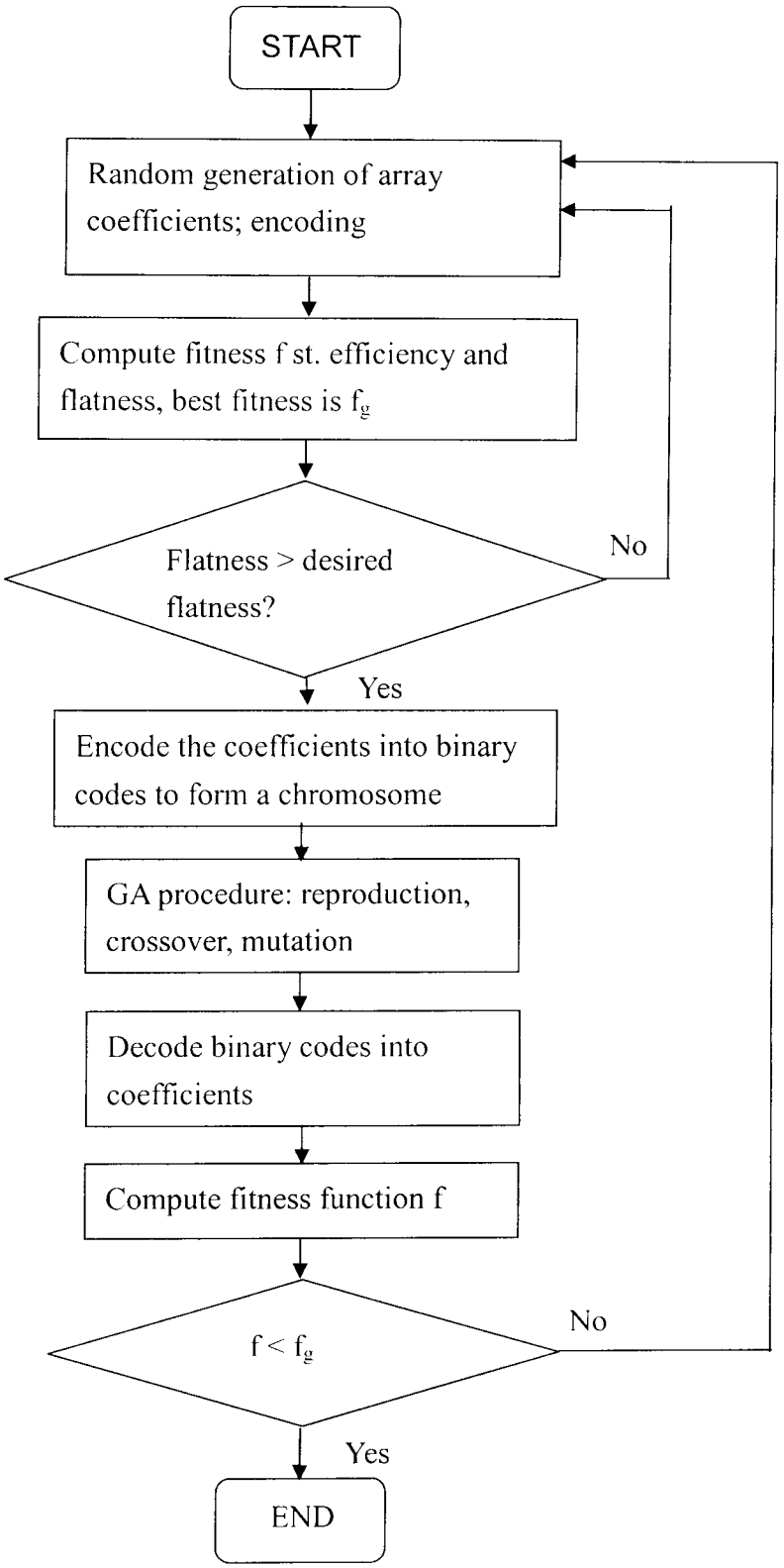

Fig. 5
Bai and Kuo

Parents:

Parent 1	XXX	YYY	ZZZ
Parent 2	xxx	yyy	zzz

Possible offspring:

Child 1	XXX	YYY	zzz
Child 2	xxx	yyy	ZZZ

(a)

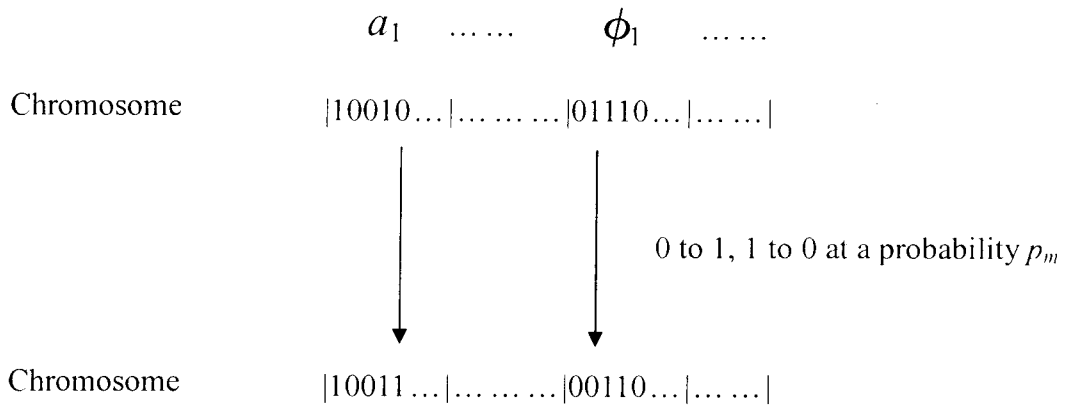

(b)

Fig. 6
Bai and Kuo

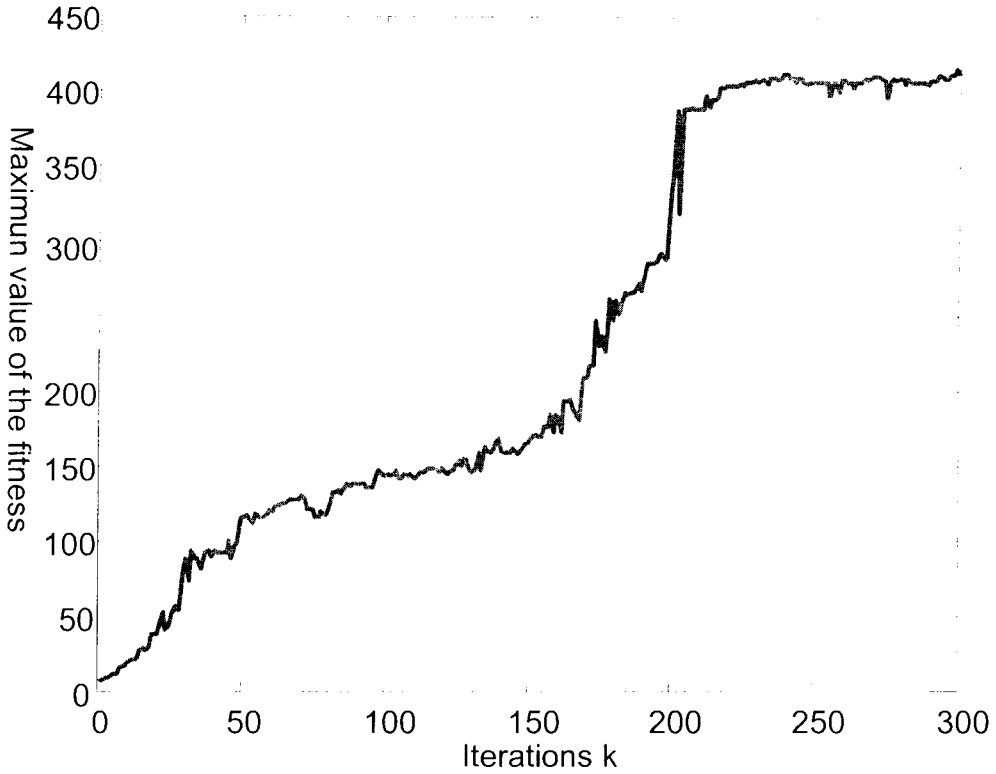

Fig. 7
Bai and Kuo

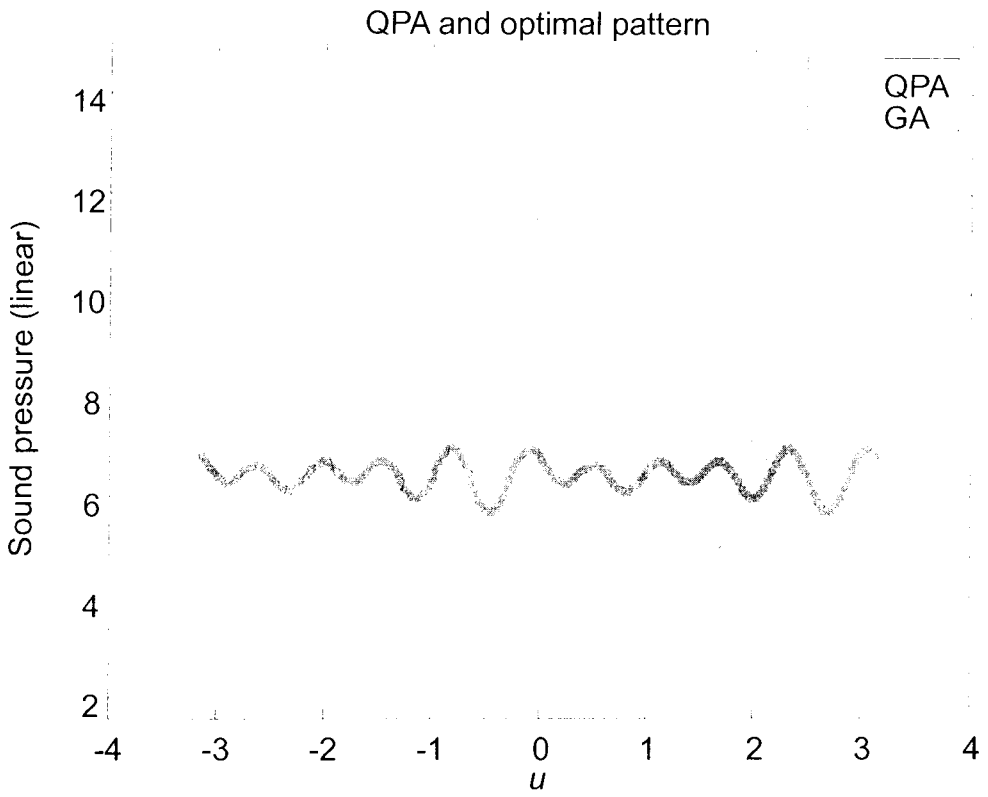

Fig. 8
Bai and Kuo

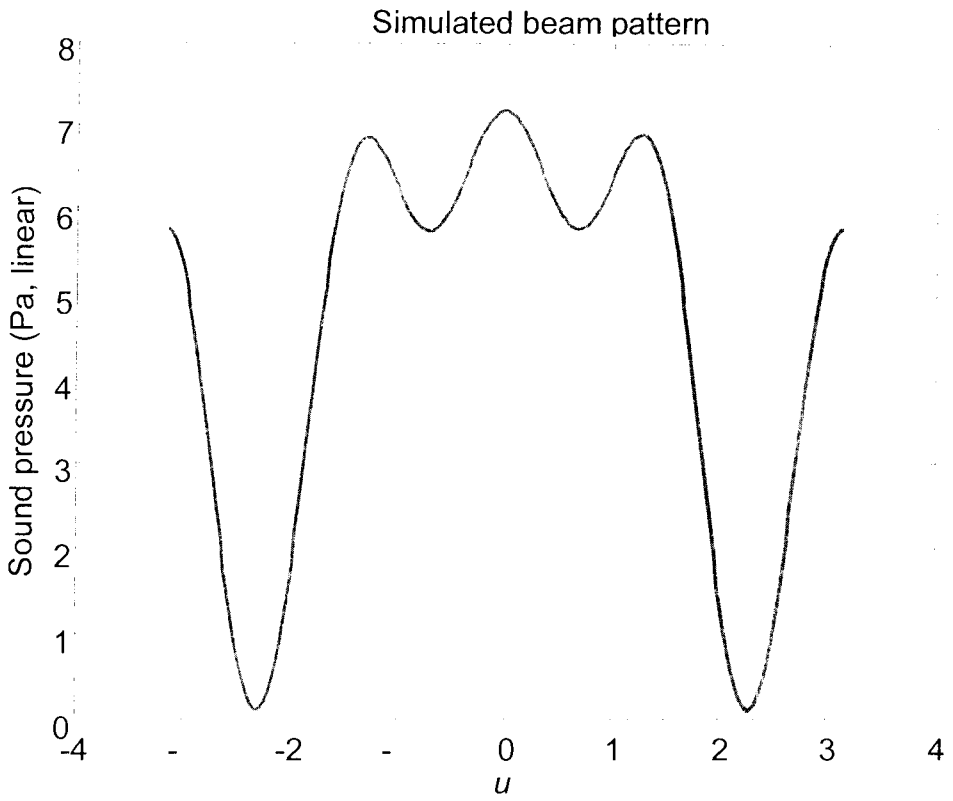

Fig. 9
Bai and Kuo

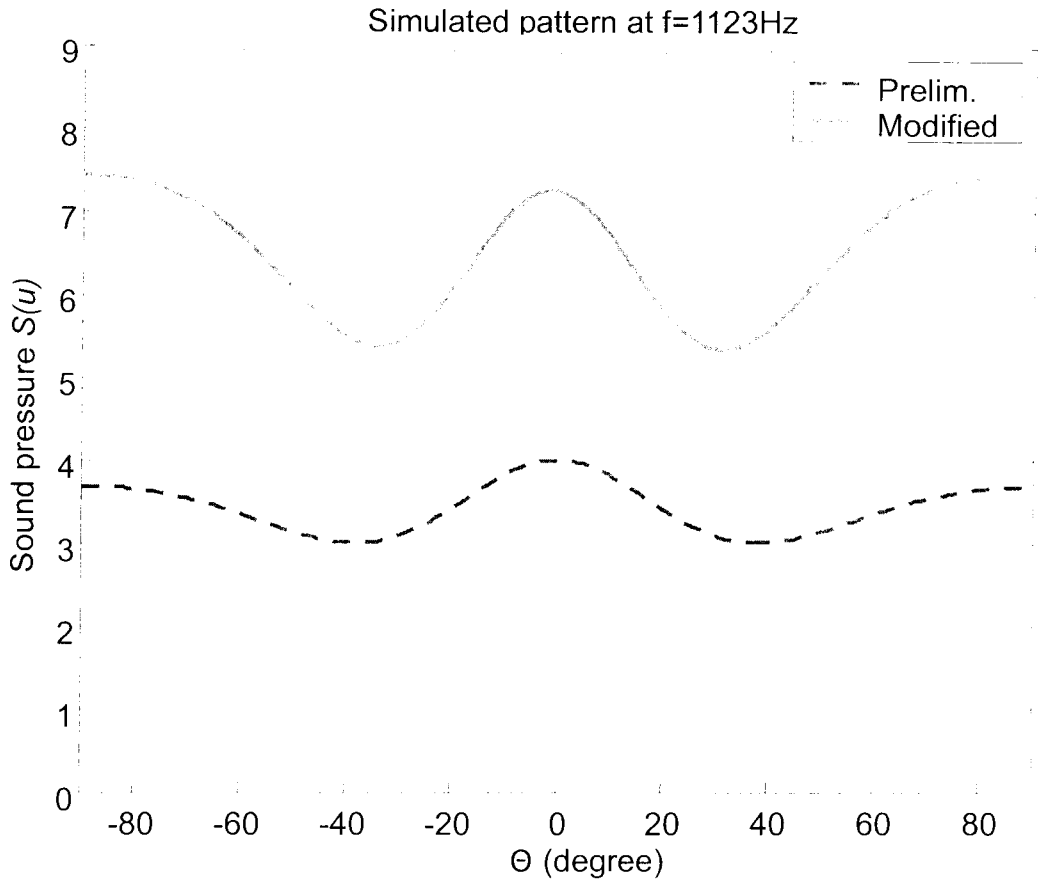

Fig. 10
Bai and Kuo

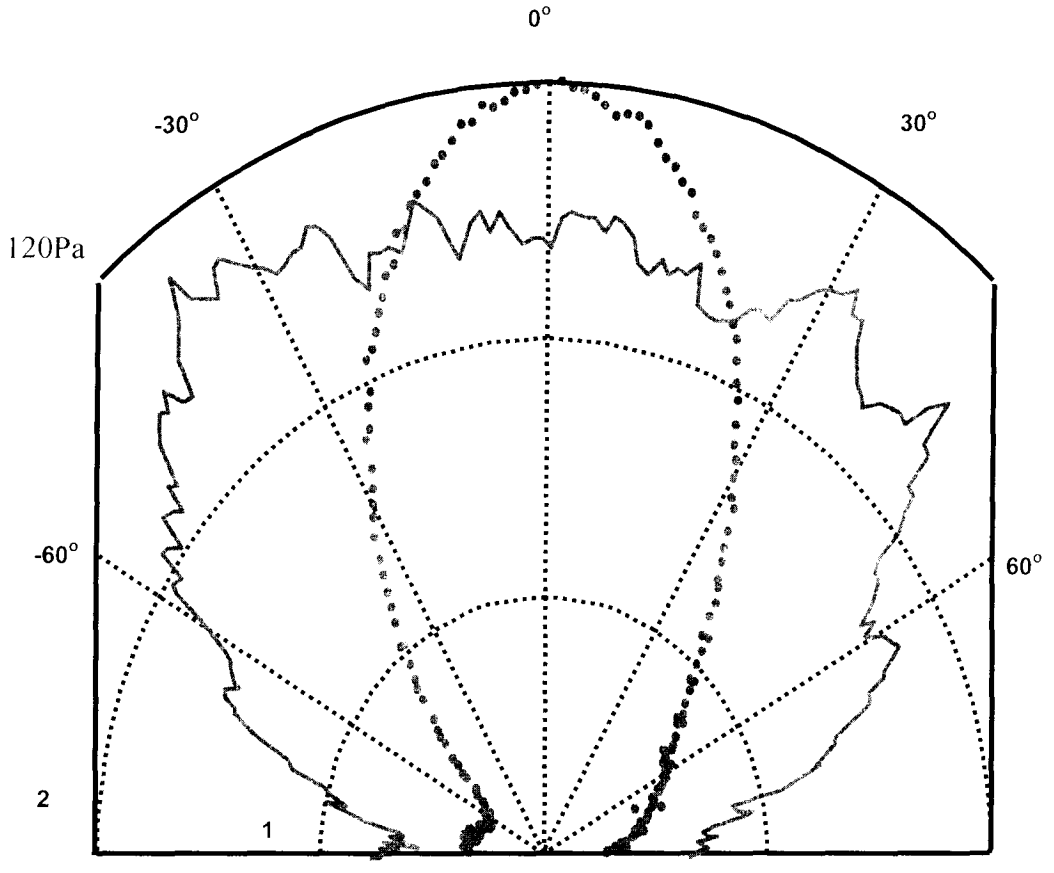

Fig. 11
Bai and Kuo

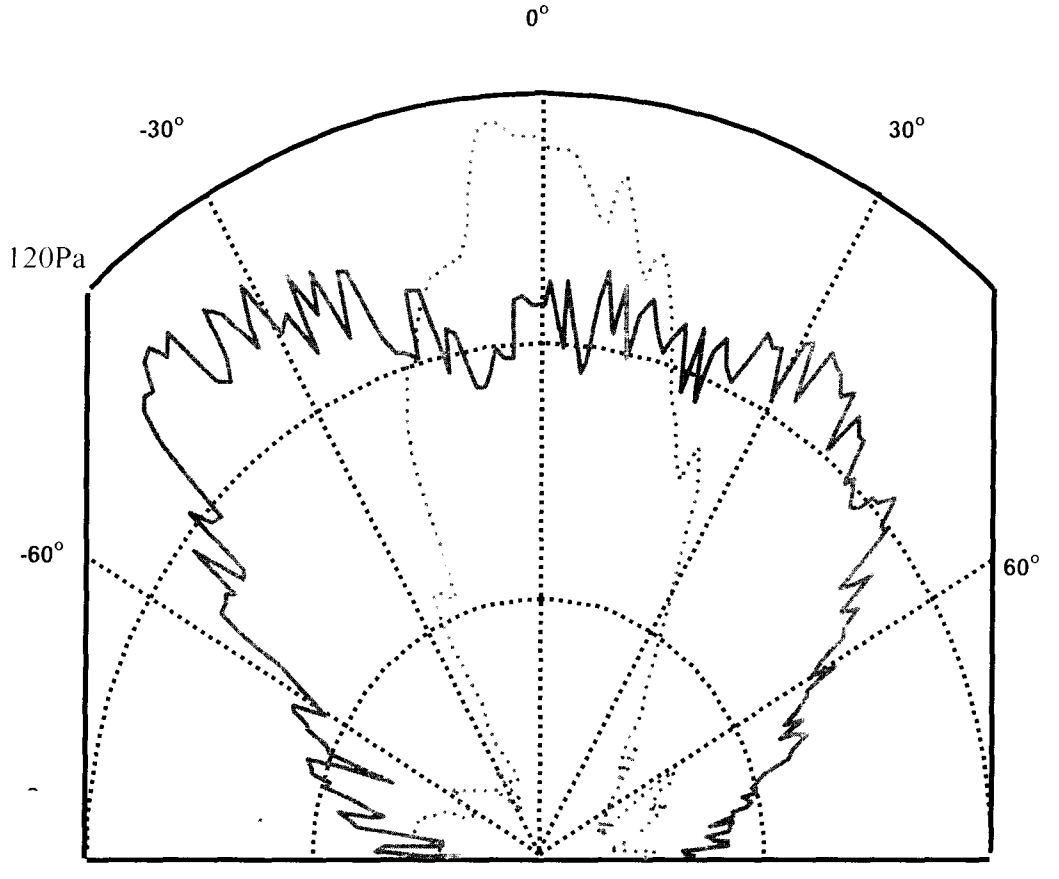

Fig. 12
Bai and Kuo

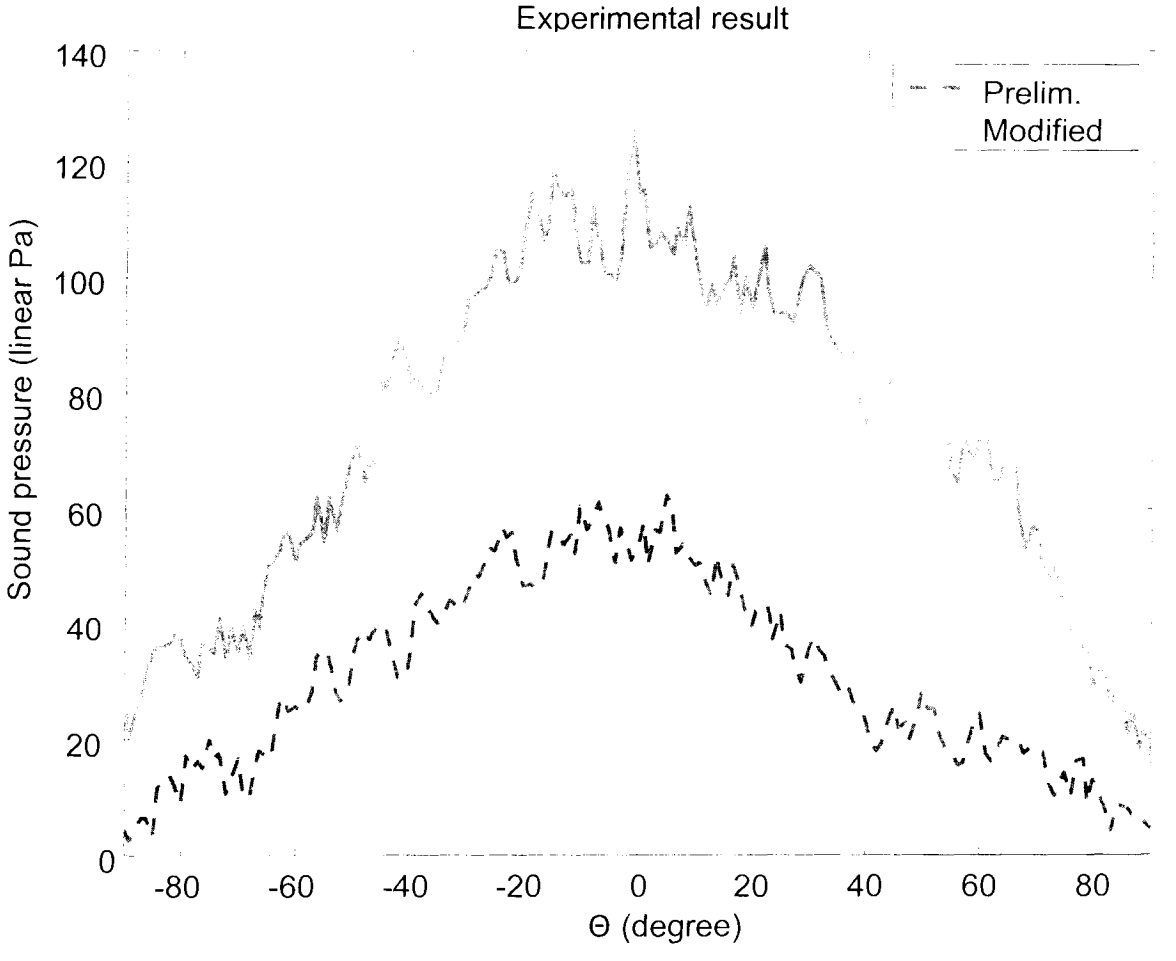

Fig. 13
Bai and Kuo

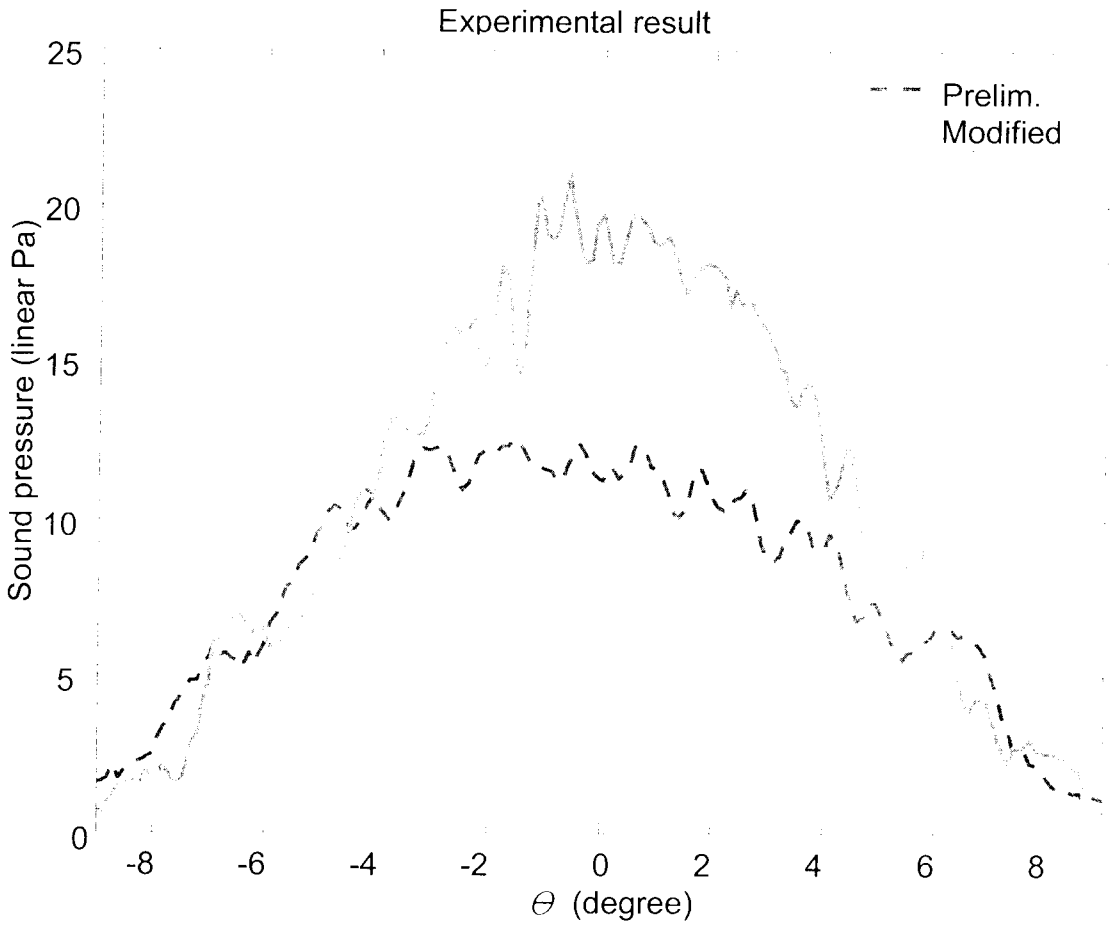

Fig. 14
Bai and Kuo